Ultrasonic Solution for Structural Health Monitoring Using Embedded Non-Destructive Testing

SIMON A. CLÉMENT, ALICE AUBRY, AROUSA FOURATI, GRÉGOIRE MARIN, FRÉDÉRIC JEAN and FRÉDÉRIC MOSCA

ABSTRACT

A high number of actors of the space industry, including ESA (European Space Agency) and CNES (French national space agency), are engaged in a program aiming to develop future European reusable space launchers. In this context, PYTHEAS Technology develops an embedded Non-Destructive Testing (eNDT) solution aiming to ensure that strategic parts of the launcher are free of damage before a new launch. Structural damage can be detected, localized and characterized using a network of piezoelectric transmitters/receivers, embedded in the structure, which send and receive guided waves. The technique is based on a comparison between the baseline ultrasound signature of the structure and the deviation of a new ultrasound cartography from this reference. The system is tested experimentally on an aluminum honeycomb sandwich structure, specifically on a section of a payload adaptor. Detection, localization and characterization of different types of structural defects are carried out experimentally, and the performances of the system are discussed.

INTRODUCTION

Using reusable satellite launchers was proved to be feasible for the first time during the past decade. The reduction of launch costs enabled by reusing space launchers or components attracts a lot of attention and the CNES (Centre National d'Etudes Spatiales), ESA (European Space Agency) and private companies are developing the future European reusable launchers.

However, satellite launchers are subject to extreme mechanical and thermal loading, making it difficult to ensure they are safe to take off again after landing. PYTHEAS Technology is developing, with CNES, an embedded non-destructive testing (NDT) system, spread over the launcher's structure, capable of detecting, localizing and characterizing defects, thus performing structural health monitoring (SHM).

Authors' affiliation: PYTHEAS Technology, 100 Impasse des Houillères, Meyreuil, France

Embedded SHM methods for damage detection can use the propagation of Lamb waves in structures and are then based on a network of sensors mechanically linked and highly coupled to the structure to be investigated. They are mainly of 2 types: Optical Fiber Bragg grating (FBG) sensors [1-3] and piezoelectric wafer networks [4-6].

The latter has several advantages over the former:

- It allows the use of active and passive methods, due to the reversibility of the piezoelectric effect, allowing both to generate Lamb waves and to sense them [4-6].
- Moreover, by beamforming techniques, it allows the imaging (thus localization) of defects and their characterization [4,7,8,9].

Several methods of investigation can be implemented using an array of piezoelectric sensors, among which:

- Passive methods using spectral analysis of the vibrations of the structure [10,11]
- The so-called acoustic emission (AE) method for fault initiation detection [12]
- The active method for imaging and damage characterization [4,7,8,9]

The passive method is limited to structures subject to ambient vibrations, which are used to analyze the modal behavior of the structure. The AE method only applies to the appearance of a damage or a shock and does not allow to scan a structure at any given time. Only the active method allows, by Lamb wave generation, to characterize the structure at any time, as much as necessary.

Damage detection and localization using Lamb Waves is now a proven technology, as shown by the theoretical and experimental work in the book [4] and the extensive review given in [5]. It combines several methods:

- Wave mode tuning allows the excitation of a single mode by selecting a “sweet spot”, a spectral zone where the amplitude of a mode is large in front of the others [4].
- On the hardware side, interdigitated transducers allow to select the modes excited, thanks to the periodicity of their patterns [13].
- Signal processing allows a comparison to a reference acoustic response (also called baseline), to distinguish the general evolution of the signal from the localized appearance of a defect. Several approaches exist: removal of common trends by cointegration [14,15], time-frequency processing and time of flight use [16].
- A damage index (DI) is then calculated based on the measurement of the deviation from the baseline response. It is generally evaluated between 0 and 1 and makes it possible to assess the severity of the defect [17].
- On top of detection, identification and monitoring of the defect can be achieved by methods such as the delay and sum method [18] or time reversal [19], to name a few.

In the present article, damage detection and localization are applied to an aluminum honeycomb sandwich structure. Research was performed on analyzing the inside of honeycomb structures by other teams [7,20], however the present study focuses on detecting and localizing defects in the skins of the honeycomb sandwich structure.

The system presented can be embedded on a structure and perform ultrasound inspection, detecting, localizing and characterizing defects in place. For this reason, it is between embedded SHM methods and classic ultrasound NDT performed by an operator, and is thus called embedded NDT (eNDT).

In the first section of the article, the case study is detailed, and the detection and localization methodologies used are presented. In the second section, experimental results are presented on a reduced-scale specimen. In the third section, experimental results are presented on the section of a satellite launcher payload adaptor. Finally, conclusions and perspectives are drawn.

CASE STUDY AND METHODOLOGY

Case Study

The detection and localization methodologies were tested on an aluminum honeycomb sandwich structure, specifically a portion of a payload adaptor. This structure is composed of two aluminum skins and an internal aluminum honeycomb.

The goal of the eNDT system is to identify damage in the skins, such as holes, scratches, or recesses, which could be created by shocks or the buckling of the structure. Delamination between the skins and the honeycomb will also be studied in the future.

During the study, preliminary tests were carried out on reduced-scale specimens (30x30cm) to estimate the effect of the honeycomb on the Lamb wave propagation and validate the methodology, as shown in Figure 1.

The transducers used are piezoelectric patches, used both as emitters and receivers. The patches are DuraAct P-876.SP1 from PI (Physik Instrumente), their overall dimensions are 16x13x0.5mm, and the piezoelectric PZT (PIC255) ceramic's dimensions are 10x10x0.2mm.

The excitation signal was selected to have a central frequency of 250kHz and a bandwidth of 250kHz, allowing to solicit only fundamental modes A0 and S0, eliminating higher harmonics and simplifying signal processing.

Simple pitch-catch tests were carried out, both for the simple aluminum plate and the one with honeycomb. Both specimens have the same aluminum material, same thickness, and the patches are positioned identically.

Simple pitch-catch tests were carried out, both for the simple aluminum plate and the one with honeycomb. Both specimens have the same aluminum material, same thickness, and the patches are positioned identically.

The signals received on the receiving patch are given in Figure 2 for both configurations, for a 10V peak-peak voltage applied to the emitting patch.

In Figure 2, the first strong signal received is the symmetrical Lamb wave S0, closely followed by the asymmetrical Lamb wave A0. The following segments of the signal are echoes, reflected by the sides of the panels travelling further through the aluminum plate or skin and thus subject to more attenuation.

The honeycomb is glued to the aluminum skins, and this polymer glue generates damping, decreasing the amplitude of the acoustic signal.

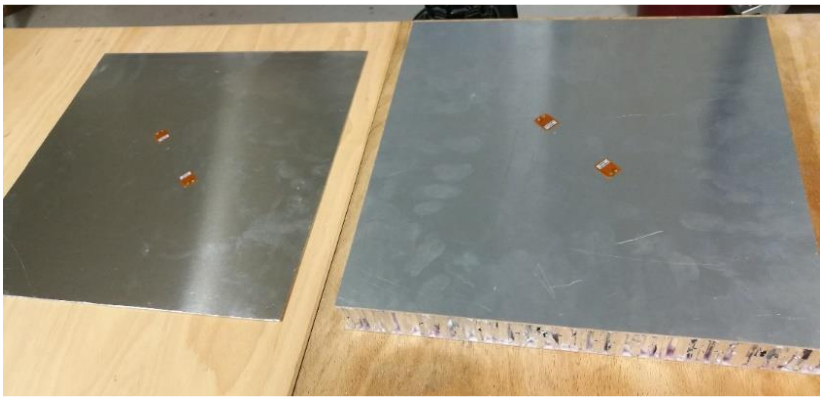

Figure 1. Reduced-scale specimen used to validate the methodology, without honeycomb on the left, and with honeycomb on the right.

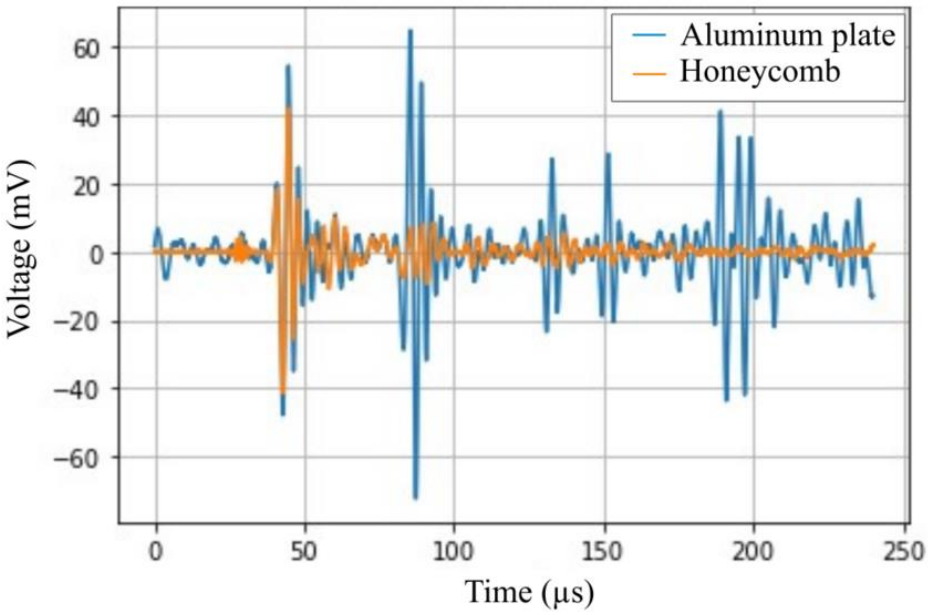

Figure 2. Signals received for a simple aluminum plate, and on the skin of the plate with honeycomb.

Signal Processing for Damage Detection

The detection methodology uses a comparison between a baseline acoustic signature of the pristine structure and the one of the structure with defects. Deviation from the baseline signature is quantified by calculating the damage index (DI).

The DI can be computed in different ways. Popular metrics, described below, are the root mean square deviation (RMSD), the mean absolute percentage deviation (MAPD), the covariance (Cov) and the correlation coefficient deviation (CCD) [4]:

$$RMSD = \sqrt{\frac{\sum_N (S_i - S_i^0)^2}{\sum_N (S_i^0)^2}} \tag{1}$$

$$MAPD = \sum_N \left| \frac{S_i - S_i^0}{S_i^0} \right| \tag{2}$$

$$Cov = \frac{1}{N-1} \sum_N (S_i - \bar{S})(S_i^0 - \overline{S^0}) \tag{3}$$

$$CCD = 1 - \frac{\sum_N (S_i - \bar{S})(S_i^0 - \overline{S^0})}{\sqrt{\sum_N (S_i - \bar{S})^2 \sum_N (S_i^0 - \overline{S^0})^2}} \tag{4}$$

where N is the number of frequencies in the spectrum, S_i and S_i^0 are the spectrum coefficients respectively of the measured and baseline signals. One could also replace these coefficients by carefully chosen wavelet coefficients to obtain different metrics.

During this research, different metrics were tested, and the results presented here were obtained using the root mean square deviation computed on Fourier coefficients selected at a set of chosen frequencies. This methodology provided the highest level of reliability and repeatability for our application cases.

Signal Processing for Damage Localization

Several methods exist to localize damages. In our process, we combine imagery methods with detection methods to localize a damage. We consider that the presence of a damage on the structure can either have an echo effect or an attenuation effect, as done in [5].

As presented previously, defects are detected by comparing the signal received to baseline signals. The Hilbert transform is then applied to the signals to obtain their envelopes. The Hilbert transforms of the baseline and measured signals are then compared to obtain the timestamp corresponding to the defect, as shown in Figure 3.

Once the defect is detected and a timestamp is identified, a length is calculated knowing the speed of the S0 Lamb wave. This calculation is repeated for each pair of patches, leading to one distance per pair. An ellipse is then formed for each pair, where the patches are the focal points of the ellipse. By using several pairs of emitters and receivers, the position of the defect can be obtained at the intersection of the reconstructed ellipses.

This methodology requires a minimum of three patches to obtain a full localization, since three pairs are necessary to create three ellipses and obtain a unique point of intersection. Increasing the number of patches of course increases the precision of the method, but with a cost in terms of patch density.

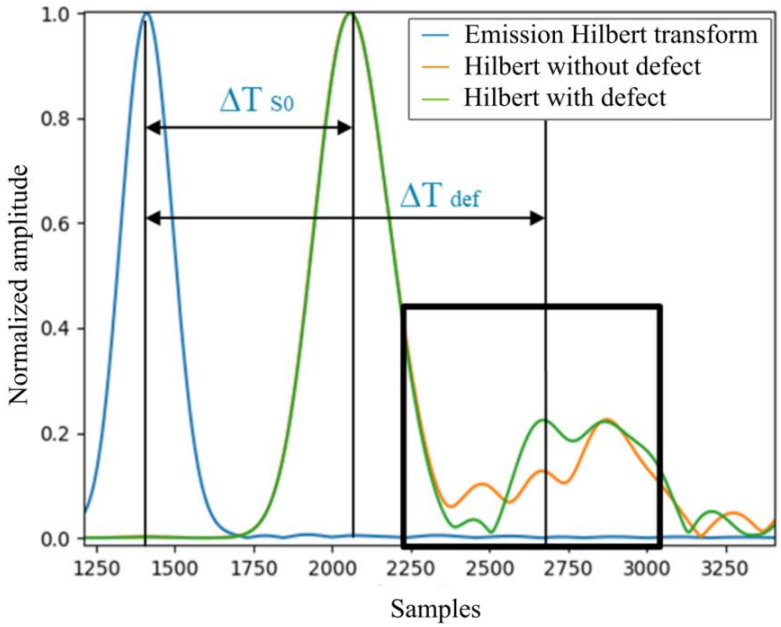

Figure 3. Hilbert transforms of the emitted signal, baseline signal and measured signal with defect. The propagation time of the symmetric S0 Lamb wave is highlighted, as well as the timestamp of the defect.

EXPERIMENTAL RESULTS ON THE REDUCED-SCALE SPECIMEN

To validate the methodology, tests were carried out on the reduced-scale honeycomb plate presented previously. A first defect, a recess, was added using a hydraulic press. The damage index was calculated using the methodology described previously, providing a measure of the difference between the signals. Figure 4 shows the damage indices measured with the pristine specimen on four different days.

The horizontal line represents the damage index limit set to identify the appearance of a damage. The two last measurements were obtained with the recess, generating a damage index well above the detection threshold.

After validating the detection of the recess, a hole was drilled in the skin of the honeycomb structure. Tests were performed with increasing diameters to evaluate if the damage index is modified by the size of the hole.

The honeycomb structure with the recess then becomes the baseline structure. Figure 5 gives the damage indices obtained with the recess alone (Ref 1 to 4) and with different hole diameters (4mm, 6mm and 8mm).

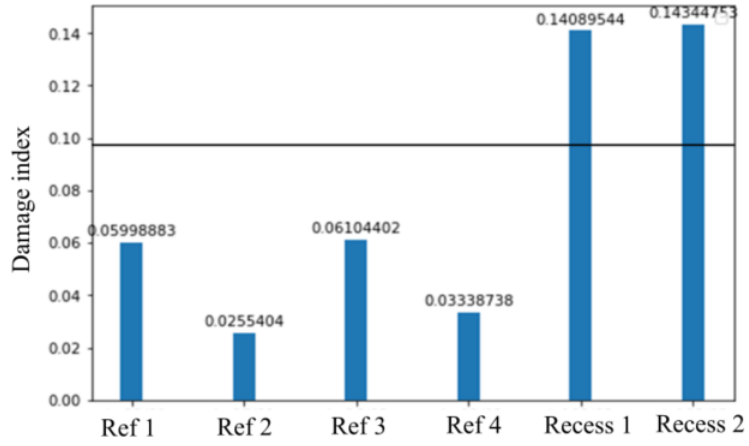

Figure 4. Damage index measured at four different dates before adding a damage (Ref 1 to 4), and with the recess (Recess 1 and 2). The horizontal black line represents the damage detection threshold.

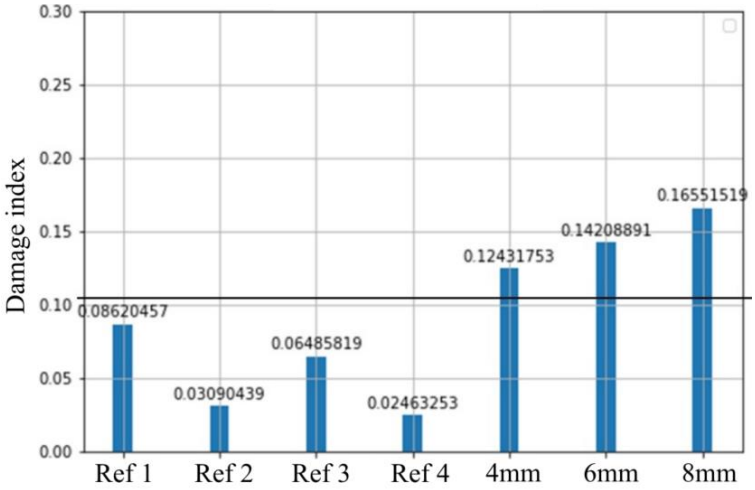

Figure 5. Damage indices obtained with the recess alone (ref 1 to 4) and with a hole of increasing diameter added (4mm, 6mm and 8mm).

First, these results show the capability of the system to detect holes, as their damage indices exceed the detection threshold. Second, the damage index increases with the hole size. Being able to quantify the magnitude of the damage is a great addition to the detection and localization capabilities of the system.

EXPERIMENTAL RESULTS ON THE FULL-SCALE STRUCTURE

The payload adaptor section used for the full-scale tests measures 2m by 3m approximately. A network of 5 piezoelectric patches is installed on the structure to instrument a portion measuring 60cm by 60cm. Three defects are then added on the top skin of the structure, as shown in Figure 6: a hole of diameter 4mm initially, then increased progressively to 8mm, a scratch on the surface 30mm long, 1mm wide and 0.5mm deep, and a recess 2mm deep with a diameter of 15mm.

Different sets of patches are used to localize each defect: P2, P3 and P5 for the hole, P3, P4 and P5 for the scratch, and P1, P2, P3 and P4 for the recess. The methodology presented previously was applied to these different groups of patches, leading to the results presented in Figure 7.

The defects are well localized by the method, although an error appears on the localization of the scratch. This error could come from the shape of the scratch, which is further away from a punctual disturbance on the propagation of the acoustic waves.

The uncertainty of the localization method (represented by yellow squares in Figure 7) comes from several factors, including the fact that the patches are rectangles instead of punctual sources and receivers, that the signals have noise, and that the structure is curved and not necessarily homogenous (especially regarding the glue thickness between the skin and the honeycomb).

The capability to detect these three types of defects on the skin of an aluminum honeycomb sandwich structure was thus validated. Localization of these defects was also demonstrated, although the accuracy can be improved for certain types of defects.

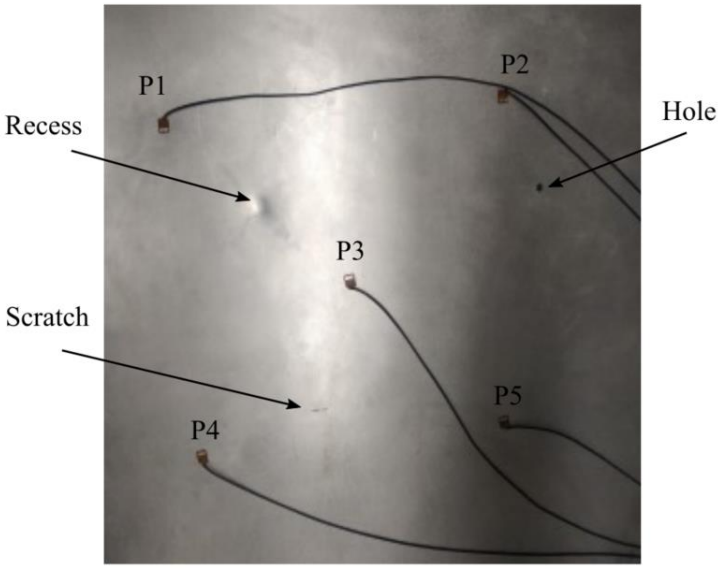

Figure 6. Picture of the full-scale honeycomb structure with the three defects created. The piezoelectric patches are numbered P1 to P5.

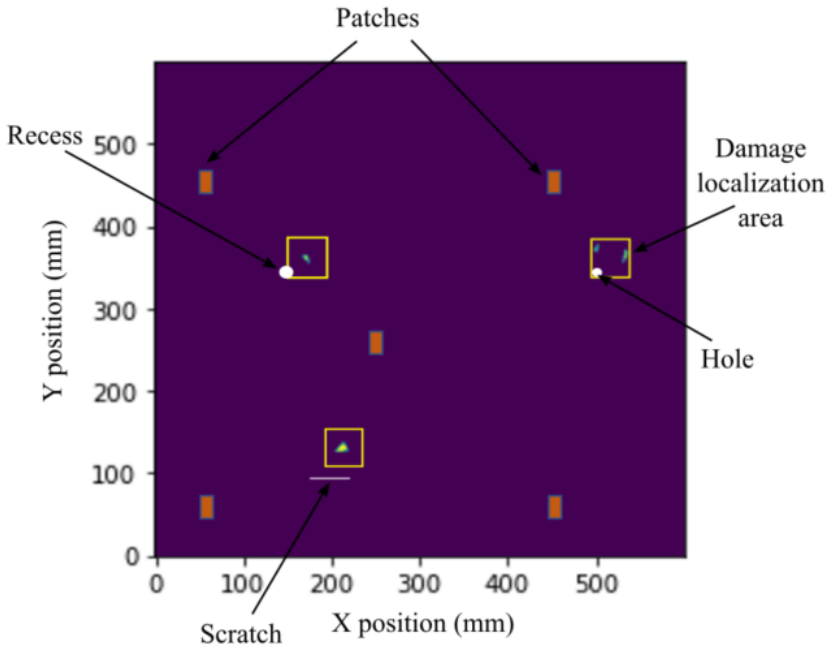

Figure 7: Result of the detection and localization of the three defects generated on the full-scale honeycomb structure. The colored areas correspond to areas where several ellipses intersect. The yellow squares represent an estimation of the localization uncertainty of the methodology.

CONCLUSION

A methodology to detect and localize structural defects using a network of piezoelectric emitters and receivers is presented. The network is embedded on the structure and uses a baseline acoustic signature to detect defects. Localization is carried out using an algorithm based on the formation of ellipses around each pair of patches.

This detection and localization methodology is applied to an aluminum honeycomb sandwich structure, first on a reduced-scale specimen, then on the section of a satellite launcher payload adaptor. A hole, a scratch on the surface of the skin and a recess were detected and localized, proving the performance of the methodology.

Future work includes the detection of delamination between layers of composites structures, which is an important goal of SHM applied to composite materials. The insensitivity to ambient vibrations was studied but not mentioned here for conciseness, and sensitivity to temperature also under study.

Finally, the methodology needs to be applied to larger structures, including fuel reservoirs or full payload adaptors, to decrease the patch density and evaluate its industrial relevance at large scale.

ACKNOWLEDGEMENTS

The authors would like to thank the CNES (Centre National d'Etudes Spatiales) for its support, in particular David Miot, Laurent Boireau, Adrian Garcia and Marie Jacquesson, for sharing their experience and expertise, and very valuable advice. Our technology would not have reached this level of performance without their support.

REFERENCES

1. P. Antunes, H. Lima, N. Alberto, L. Bilro, P. Pinto, A. Costa, H. Rodrigues, J.L. Pinto, R. Nogueira, H. Varum, P.S. André, Optical Sensors Based on Fiber Bragg Gratings for Structural Health Monitoring, New Developments in Sensing Technology for Structural Health Monitoring, Lecture Notes in Electrical Engineering 96, Springer, Berlin, Heidelberg, 2011.
2. Y. Qiu, Q. Wang, H. Zhao, Review on composite structural health monitoring based on fiber Bragg grating sensing principle, J. Shanghai Jiaotong Univ. 18 (2013) 129–139.
3. G. Hegde, S. Asokan, G. Hegde, Fiber Bragg grating sensors for aerospace applications: a review, ISSS J Micro Smart Syst 11 (2022) 257–275.
4. V. Giurgiutiu, Health Monitoring with Piezoelectric Wafer Active Sensors, Second Edition, Academic Press, 2014.
5. M. Philibert, K. Yao, M. Gresil, C. Soutis, Lamb waves-based technologies for structural health monitoring of composite structures for aircraft applications, European Journal of Materials 2(1) (2022) 436-474.
6. X. Qing, W. Li, Y. Wang, H. Sun, Piezoelectric Transducer-Based Structural Health Monitoring for Aircraft Applications, Sensors 19 (2019) 545.
7. A. Kulakovskyi, O. Mesnil, A. Lhémery, B. Chapuis, O. d'Almeida, Defect imaging in layered composite plates and honeycomb sandwich structures using sparse piezoelectric transducers network, J. Phys. Conf. Series 1184 (2019) 012001.
8. H. Chen, Z. Liu, B. Wu, C. He, An intelligent algorithm based on evolutionary strategy and clustering algorithm for Lamb wave defect location, Structural Health Monitoring 20(4) (2021) 2088-2109.
9. Y. Wang, L. Qiu, Y. Luo, R. Ding, A stretchable and large-scale guided wave sensor network for aircraft smart skin of structural health monitoring, Structural Health Monitoring 20(3) (2021) 861-876.
10. S. Yan, J. Wu, W. Sun, Ma H, H. Yan, Development and Application of Structural Health Monitoring System Based on Piezoelectric Sensors, International Journal of Distributed Sensor Networks (2013)
11. J. Vitola, F. Pozo, D.A. Tibaduiza, M. Anaya, Distributed Piezoelectric Sensor System for Damage Identification in Structures Subjected to Temperature Changes, Sensors 17 (2017) 1252.
12. S. Masmoudi, A. E. Mahi, S. Turki, Use of piezoelectric as acoustic emission sensor for in situ monitoring of composite structures, Composites Part B. Engineering 80 (2015) 307-320.
13. T. Stepinski, M. Mańka, A. Martowicz, Interdigital lamb wave transducers for applications in structural health monitoring, NDT & E International 86 (2017) 199–210.
14. E.J. Cross, K. Worden, Q. Chen, Cointegration: A novel approach for the removal of environmental trends in structural health monitoring data, Proceedings of the Royal Society A: Mathematical, Physical and Engineering Sciences 467(2133) (2011) 2712–2732.
15. E.J. Cross, G. Manson, K. Worden, S.G. Pierce, Features for damage detection with insensitivity to environmental and operational variations, Proceedings of the Royal Society A: Mathematical, Physical and Engineering Sciences 468(2148) (2012) 4098–4122.
16. C.S. Wang, F.-K. Chang, Diagnosis of impact damage in composite structures with built-in piezoelectrics network, Proceedings of SPIE Smart Structures and Materials: Smart Electronics and MEMS 3990, Newport Beach, USA, 2000.
17. V. Memmolo, E. Monaco, N.D. Boffa, L. Maio, F. Ricci, Guided wave propagation and scattering for structural health monitoring of stiffened composites, Composite Structures 184 (2018) 568–580.
18. F. Yan, R.L. Royer, J.L. Rose, Ultrasonic guided wave imaging techniques in structural health monitoring, Journal of Intelligent Material Systems and Structures 21(3) (2010) 377–384.
19. L. Qiu, M. Liu, X. Qing, S. Yuan, A quantitative multidamage monitoring method for large-scale complex composite, Structural Health Monitoring 12(3) (2013) 183–196.
20. E. Balmès, M. Guskov, J.-P. Bianchi, Validation and verification of FE models of piezo based SHM systems, ISMA International Conference on Noise and Vibration Engineering, Leuven, Belgium, 2016.